



TECHNISCHE
UNIVERSITÄT
WIEN

FWF Österreichischer
Wissenschaftsfonds

$\int dk \Pi$

Doktoratskolleg
Particles and Interactions

Jet momentum broadening beyond the jet quenching parameter from QCD kinetic theory

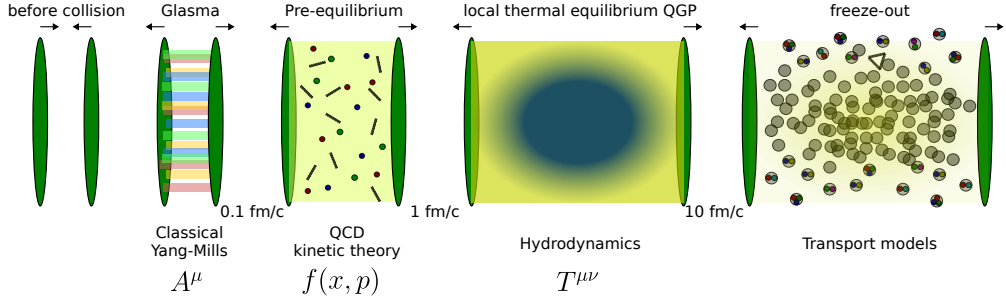
2303.12595 & 2312.00447 with K. Boguslavski, A. Kurkela, T. Lappi, J. Peuron
and based on work in preparation with Alois Altenburger & Kirill Boguslavski

Florian Lindenbauer

TU Wien

23.09.2024, Hard Probes 2024, Nagasaki, Japan

Time-evolution of the QGP in heavy-ion collisions



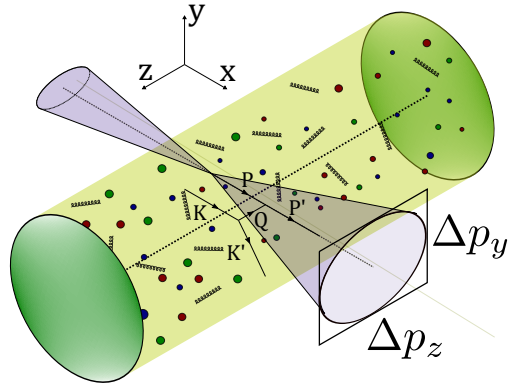
Interested in pre-equilibrium stages (“Initial stages”)

→ **QCD out of equilibrium**

[Rev.Mod.Phys. 93 (2021) [Berges, Heller, Mazeliauskas, Venugopalan]]

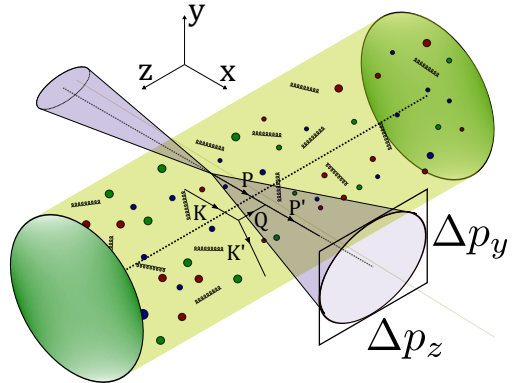
How can we study the initial stages?

- To study initial stages
→ very **energetic** or **heavy** probes
- Here depicted: **jets**



How can we study the initial stages?

- To study initial stages
→ very **energetic** or **heavy** probes
- Here depicted: **jets**
 - **Highly energetic partons**
created in initial collision
 - Splits into many particles
→ then measured in the detectors
 - Imprints of **medium interactions**



- **Energy loss** dominated by **gluon radiation**

- **Energy loss** dominated by **gluon radiation**
- Depends on effective propagator
Input: **dipole cross section**

$$C(\mathbf{b}) = \int \frac{d^2\mathbf{q}_\perp}{(2\pi)^2} C(\mathbf{q}_\perp) \left(1 - e^{i\mathbf{b}\cdot\mathbf{q}_\perp}\right)$$

$$C(\mathbf{q}_\perp) = (2\pi)^2 \frac{d\Gamma^{\text{el}}}{d^2\mathbf{q}_\perp}$$

See also JHEP 07 (2020) [Andres, Apolinário, Dominguez], JHEP 10 (2021) [Moore, Schlichting, Schlusser, Soudi], PRD 105 (2022) [Schlichting, Soudi]

- **Energy loss** dominated by **gluon radiation**
- Depends on effective propagator
Input: **dipole cross section**

$$C(\mathbf{b}) = \int \frac{d^2\mathbf{q}_\perp}{(2\pi)^2} C(\mathbf{q}_\perp) \left(1 - e^{i\mathbf{b}\cdot\mathbf{q}_\perp}\right)$$

$$C(\mathbf{q}_\perp) = (2\pi)^2 \frac{d\Gamma^{\text{el}}}{d^2\mathbf{q}_\perp}$$

See also JHEP 07 (2020) [Andres, Apolinário, Dominguez], JHEP 10 (2021) [Moore, Schlichting, Schlusser, Soudi], PRD 105 (2022) [Schlichting, Soudi]

- **Harmonic approximation:** (small b limit)
Dependence on single medium parameter \hat{q}

$$C(\mathbf{b}) \approx \frac{1}{4} \hat{q} \mathbf{b}^2 + \dots$$

“**Jet quenching parameter**”

Jet energy loss through medium-induced radiation

- **Energy loss** dominated by **gluon radiation**
- Depends on effective propagator
Input: **dipole cross section**

$$C(\mathbf{b}) = \int \frac{d^2 \mathbf{q}_\perp}{(2\pi)^2} C(\mathbf{q}_\perp) \left(1 - e^{i\mathbf{b} \cdot \mathbf{q}_\perp}\right)$$

$$C(\mathbf{q}_\perp) = (2\pi)^2 \frac{d\Gamma^{\text{el}}}{d^2 q_\perp}$$

See also JHEP 07 (2020) [Andres, Apolinário, Dominguez], JHEP 10 (2021) [Moore, Schlichting, Schlusser, Soudi], PRD 105 (2022) [Schlichting, Soudi]

- **Harmonic approximation:** (small b limit)
Dependence on single medium parameter \hat{q}

$$C(\mathbf{b}) \approx \frac{1}{4} \hat{q} \mathbf{b}^2 + \dots$$

“Jet quenching parameter”

- Quantifies **momentum broadening**

$$\hat{q} = \frac{d\langle p_\perp^2 \rangle}{dL} = \frac{d\langle p_\perp^2 \rangle}{dt} = \int d^2 q_\perp q_\perp^2 \frac{d\Gamma^{\text{el}}}{d^2 q_\perp}$$

Jet energy loss through medium-induced radiation

- **Energy loss** dominated by **gluon radiation**

- Depends on effective propagator

Input: **dipole cross section**

$$C(\mathbf{b}) = \int \frac{d^2 \mathbf{q}_\perp}{(2\pi)^2} C(\mathbf{q}_\perp) \left(1 - e^{i\mathbf{b} \cdot \mathbf{q}_\perp}\right)$$

$$C(\mathbf{q}_\perp) = (2\pi)^2 \frac{d\Gamma^{\text{el}}}{d^2 q_\perp}$$

See also JHEP 07 (2020) [Andres, Apolinário, Dominguez], JHEP 10 (2021) [Moore, Schlichting, Schlusser, Soudi], PRD 105 (2022) [Schlichting, Soudi]

- **Harmonic approximation**: (small b limit)
Dependence on single medium parameter \hat{q}

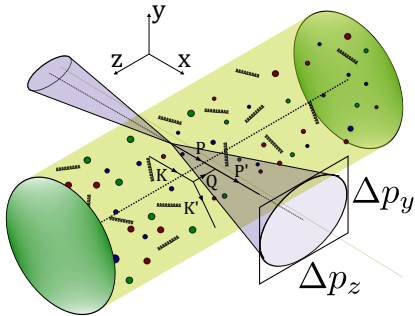
$$C(\mathbf{b}) \approx \frac{1}{4} \hat{q} \mathbf{b}^2 + \dots$$

“**Jet quenching parameter**”

- Quantifies **momentum broadening**

$$\hat{q}^{ij} = \frac{d\langle p_\perp^i p_\perp^j \rangle}{dt} = \int d^2 q_\perp q_\perp^i q_\perp^j \frac{d\Gamma^{\text{el}}}{d^2 q_\perp}$$

$$\hat{q} = \hat{q}^{yy} + \hat{q}^{zz}$$



- **Harmonic approximation:** (small b limit)
Dependence on single medium parameter \hat{q}

$$C(\mathbf{b}) \approx \frac{1}{4} \hat{q} \mathbf{b}^2 + \dots$$

“Jet quenching parameter”

- Quantifies **momentum broadening**

$$\hat{q}^{ij} = \frac{d\langle p_{\perp}^i p_{\perp}^j \rangle}{dt} = \int d^2 q_{\perp} q_{\perp}^i q_{\perp}^j \frac{d\Gamma^{\text{el}}}{d^2 q_{\perp}}$$

$$\hat{q} = \hat{q}^{yy} + \hat{q}^{zz}$$



Physics Letters B

Volume 803, 10 April 2020, 135318



Jet quenching as a probe of the initial stages in heavy-ion collisions ☆

Carlota Andres^a , Néstor Armesto^b , Harri Niemi^{c,d} , Risto Paatelainen^{e,d} ,
Carlos A. Salgado^b

ABSTRACT

Jet quenching provides a very flexible variety of observables which are sensitive to different energy- and time-scales of the strongly interacting matter created in heavy-ion collisions. Exploiting this versatility would make jet quenching an excellent chronometer of the yoctosecond structure of the evolution process. Here we show, for the first time, that a combination of jet quenching observables is sensitive to the initial stages of heavy-ion collisions, when the approach to local thermal equilibrium is expected to happen. Specifically, we find that in order to reproduce at the same time the inclusive particle production suppression, R_{AA} , and the high- p_T azimuthal asymmetries, v_2 , energy loss must be strongly suppressed for the first ~ 0.6 fm. This exploratory analysis shows the potential of jet observables, possibly more sophisticated than the ones studied here, to constrain the dynamics of the initial stages of the evolution.

© 2020 The Author(s). Published by Elsevier B.V. This is an open access article under the CC BY license (<http://creativecommons.org/licenses/by/4.0/>). Funded by SCOAP³.

Estimates of \hat{q}

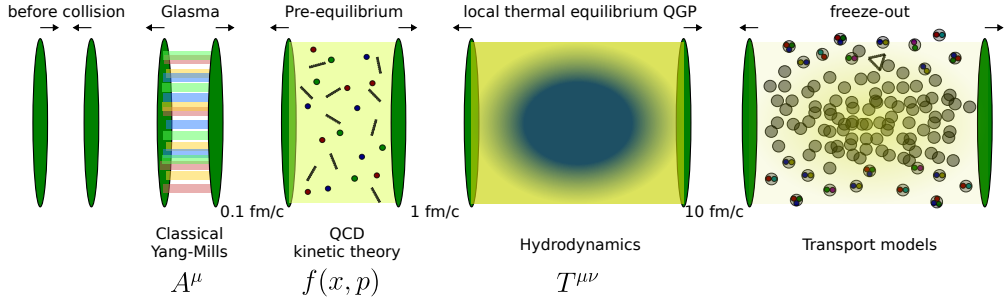
A B S T R A C T

Jet quenching provides a very flexible variety of observables which are sensitive to different energy- and time-scales of the strongly interacting matter created in heavy-ion collisions. Exploiting this versatility would make jet quenching an excellent chronometer of the yoctosecond structure of the evolution process. Here we show, for the first time, that a combination of jet quenching observables is sensitive to the initial stages of heavy-ion collisions, when the approach to local thermal equilibrium is expected to happen. Specifically, we find that in order to reproduce at the same time the inclusive particle production suppression, R_{AA} , and the high- p_T azimuthal asymmetries, v_2 , energy loss must be strongly suppressed for the first ~ 0.6 fm. This exploratory analysis shows the potential of jet observables, possibly more sophisticated than the ones studied here, to constrain the dynamics of the initial stages of the evolution.

© 2020 The Author(s). Published by Elsevier B.V. This is an open access article under the CC BY license (<http://creativecommons.org/licenses/by/4.0/>). Funded by SCOAP³.

$\hat{q} = 0$ during initial stages [Phys.Lett.B 803 (2020) [Andres, Armesto, Niemi, Paatelainen, Salgado]]

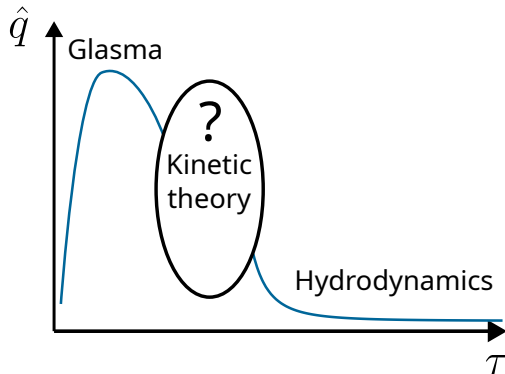
Estimates of \hat{q}



- Studies find initial stages $\hat{q}(\tau < 0.6 \text{ fm}) \equiv 0$ needed for description of jet v_2 and R_{AA} ¹
- However, studies in the initial Glasma stage find \hat{q} very large²
- **Goal: \hat{q} during hydrodynamization**
→ between Glasma and hydro
- **Question:**
Supports large Glasma values?

¹[Phys.Lett.B 803 (2020) [Andres, Armesto, Niemi, Paatelainen, Salgado]]

²[Phys.Lett.B 810 (2020) [Ipp, Müller, Schuh], Phys.Rev.C 105 (2022) [Carrington, Czajka, Mrowczynski], Phys.Rev.D 107 (2023) [Avramescu, Baran, Greco, Ipp, Müller, Ruggieri]]

Schematic overview of \hat{q} evolution

Effective kinetic theory description of the QGP

- Plasma without quarks
- Gluons with **distribution function** $f(t, \mathbf{p})$

- Azimuthal symmetry around beam axis \hat{z} ,
Bjorken expansion, homogeneous in transverse plane

³[JHEP 01 (2003) [Arnold, Moore, Yaffe], Int.J.Mod.Phys.E 16 (2007) [Arnold]]

Effective kinetic theory description of the QGP

- Plasma without quarks
- Gluons with **distribution function** $f(t, \mathbf{p})$
- Time evolution described by **Boltzmann equation** at leading-order³

$$(\partial_t + \mathbf{v} \cdot \nabla) f = \underbrace{\left| \begin{array}{c} \text{---} \\ \diagup \quad \diagdown \\ \text{---} \\ \text{---} \\ \diagdown \quad \diagup \\ \text{---} \end{array} \right|^2 + \left| \begin{array}{c} \text{---} \\ \text{---} \\ \text{---} \\ \text{---} \\ \text{---} \end{array} \right|^2}_{\text{Collision term}}$$

The diagram shows two squared terms representing collision processes. The first term is a red Feynman diagram with two incoming lines from the left and two outgoing lines to the right, connected by a vertical wavy line (gluon exchange). The second term is a red Feynman diagram with two incoming lines from the left and two outgoing lines to the right, connected by a horizontal wavy line (gluon exchange) that passes through a blue rectangular box representing a medium.

- Azimuthal symmetry around beam axis \hat{z} ,
Bjorken expansion, homogeneous in transverse plane

³[JHEP 01 (2003) [Arnold, Moore, Yaffe], Int.J.Mod.Phys.E 16 (2007) [Arnold]]

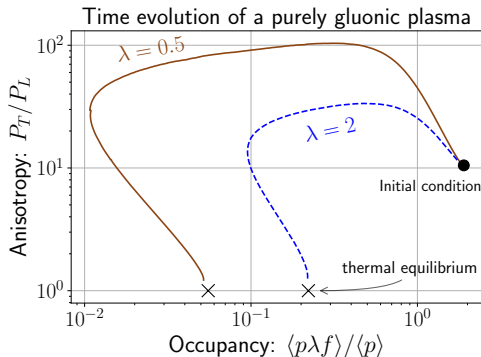
Bottom-up thermalization in heavy-ion collisions

- Initial condition⁴, with $\lambda = g^2 N_C$

$$f(p_\perp, p_z) = \frac{2A}{\lambda} \frac{\langle p_T \rangle}{\sqrt{p_\perp^2 + \xi_0^2 p_z^2}} \times \exp\left(\frac{-2}{3\langle p_T \rangle^2} (p_\perp^2 + \xi_0^2 p_z^2)\right)$$

$\xi_0 \sim$ anisotropy, $\langle p_T \rangle = 1.8Q_s$,

$Q_s \sim$ saturation scale



⁴[Phys.Rev.Lett. 115 (2015) [Kurkela, Zhu]]

⁵[Phys.Lett.B 502 (2001) [Baier, Mueller, Schiff, Son]]

Bottom-up thermalization in heavy-ion collisions

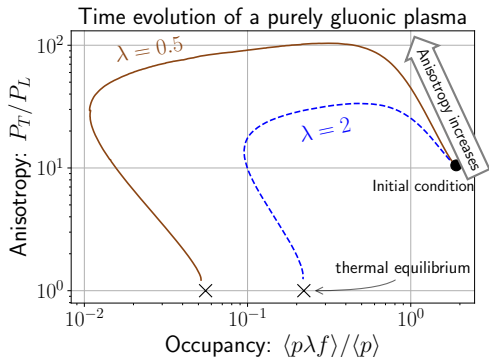
- Initial condition⁴, with $\lambda = g^2 N_C$

$$f(p_{\perp}, p_z) = \frac{2A}{\lambda} \frac{\langle p_T \rangle}{\sqrt{p_{\perp}^2 + \xi_0^2 p_z^2}} \times \exp\left(\frac{-2}{3\langle p_T \rangle^2} (p_{\perp}^2 + \xi_0^2 p_z^2)\right)$$

$\xi_0 \sim$ anisotropy, $\langle p_T \rangle = 1.8Q_s$,

$Q_s \sim$ saturation scale

- Phase 1:** Anisotropy increases



⁴[Phys.Rev.Lett. 115 (2015) [Kurkela, Zhu]]

⁵[Phys.Lett.B 502 (2001) [Baier, Mueller, Schiff, Son]]

Bottom-up thermalization in heavy-ion collisions

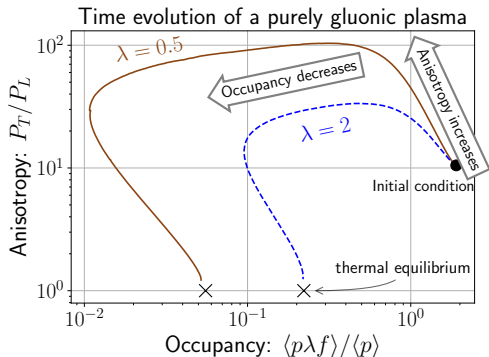
- Initial condition⁴, with $\lambda = g^2 N_C$

$$f(p_\perp, p_z) = \frac{2A}{\lambda} \frac{\langle p_T \rangle}{\sqrt{p_\perp^2 + \xi_0^2 p_z^2}} \times \exp\left(\frac{-2}{3\langle p_T \rangle^2} (p_\perp^2 + \xi_0^2 p_z^2)\right)$$

$\xi_0 \sim$ anisotropy, $\langle p_T \rangle = 1.8Q_s$,

$Q_s \sim$ saturation scale

- Phase 1:** Anisotropy increases
- Phase 2:** Occupancy decreases



⁴[Phys.Rev.Lett. 115 (2015) [Kurkela, Zhu]]

⁵[Phys.Lett.B 502 (2001) [Baier, Mueller, Schiff, Son]]

Bottom-up thermalization in heavy-ion collisions

- Initial condition⁴, with $\lambda = g^2 N_C$

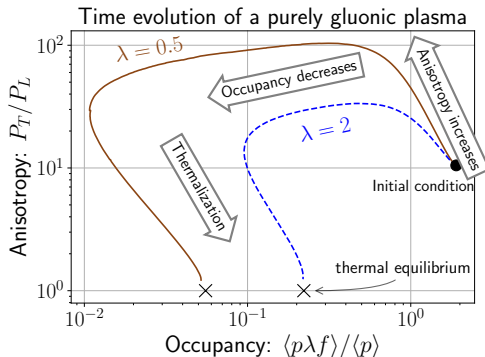
$$f(p_\perp, p_z) = \frac{2A}{\lambda} \frac{\langle p_T \rangle}{\sqrt{p_\perp^2 + \xi_0^2 p_z^2}} \times \exp\left(\frac{-2}{3\langle p_T \rangle^2} (p_\perp^2 + \xi_0^2 p_z^2)\right)$$

$\xi_0 \sim$ anisotropy, $\langle p_T \rangle = 1.8Q_s$,

$Q_s \sim$ saturation scale

- Phase 1:** Anisotropy increases
- Phase 2:** Occupancy decreases
- Phase 3:** System thermalizes at

$$\text{time}^5 \tau_{\text{BMSS}} = \left(\frac{\lambda}{12\pi}\right)^{-13/5} / Q_s$$



⁴[Phys.Rev.Lett. 115 (2015) [Kurkela, Zhu]]

⁵[Phys.Lett.B 502 (2001) [Baier, Mueller, Schiff, Son]]

Bottom-up thermalization in heavy-ion collisions

- Initial condition⁴, with $\lambda = g^2 N_C$

$$f(p_{\perp}, p_z) = \frac{2A}{\lambda} \frac{\langle p_T \rangle}{\sqrt{p_{\perp}^2 + \xi_0^2 p_z^2}} \times \exp\left(\frac{-2}{3\langle p_T \rangle^2} (p_{\perp}^2 + \xi_0^2 p_z^2)\right)$$

$\xi_0 \sim$ anisotropy, $\langle p_T \rangle = 1.8Q_s$,

$Q_s \sim$ saturation scale

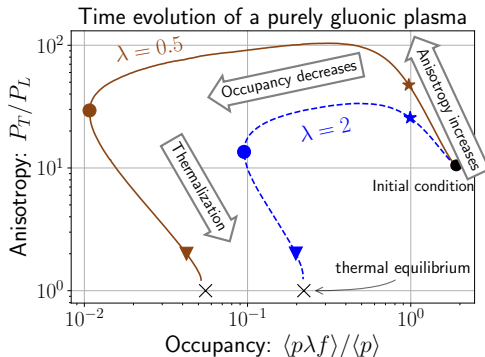
- Phase 1:** Anisotropy increases
- Phase 2:** Occupancy decreases
- Phase 3:** System thermalizes at

$$\text{time}^5 \tau_{\text{BMSS}} = \left(\frac{\lambda}{12\pi}\right)^{-13/5} / Q_s$$

Markers represent **different stages**

⁴[Phys.Rev.Lett. 115 (2015) [Kurkela, Zhu]]

⁵[Phys.Lett.B 502 (2001) [Baier, Mueller, Schiff, Son]]



- From $f(\mathbf{k})$ we obtain:

Jet momentum broadening in kinetic theory

- From $f(\mathbf{k})$ we obtain: Outgoing plasma particle

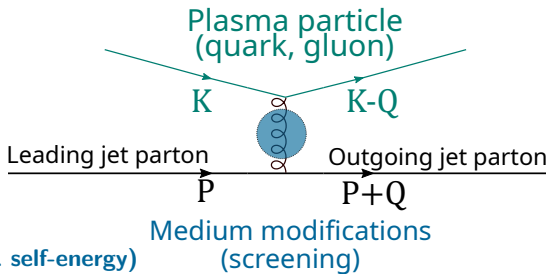
$$\hat{q}^{ij} = \int_{\substack{q_{\perp} < \Lambda \\ p \rightarrow \infty}} d\Gamma_{\text{PS}} q^i q^j |\mathcal{M}|^2 f(k) (1 + f(k'))$$

Incoming plasma particles
with momentum k

Matrix element
with medium corrections (HTL self-energy)

appropriate phase-space measure

Matrix element



Jet momentum broadening in kinetic theory

- From $f(\mathbf{k})$ we obtain:

$$C(\mathbf{q}_\perp) = \int_{p \rightarrow \infty} d\Gamma_{\text{PS}}$$

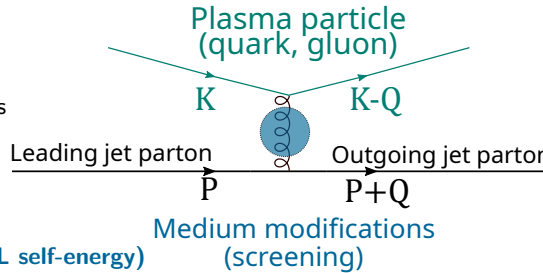
$$|\mathcal{M}|^2 f(k) (1 + f(k'))$$

Incoming plasma particles with momentum k

Matrix element with medium corrections (HTL self-energy)

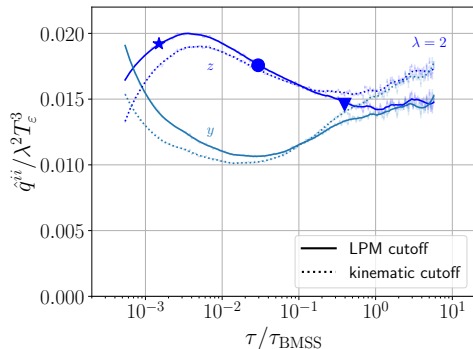
appropriate phase-space measure

Matrix element



- Cutoff models for dependence on jet energy and effective temperature

- $\Lambda_{\perp}^{\text{LPM}}(E, T_{\varepsilon}) = \zeta^{\text{LPM}} g \times (ET_{\varepsilon}^3)^{1/4}$
- $\Lambda_{\perp}^{\text{kin}}(E, T_{\varepsilon}) = \zeta^{\text{kin}} g \times (ET_{\varepsilon})^{1/2}$



[Phys.Lett.B 850 (2024) [Boguslavski, Kurkela, Lappi, FL, Peuron]]

Plot for $E = 100 \text{ GeV}$

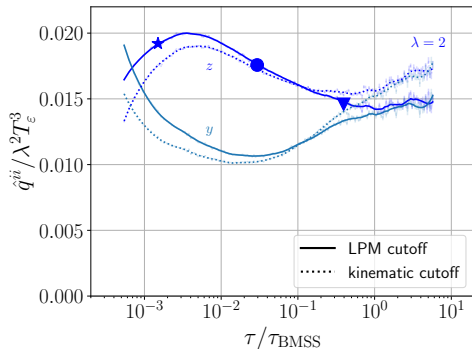
- Cutoff models for dependence on jet energy and effective temperature

- $\Lambda_{\perp}^{\text{LPM}}(E, T_{\varepsilon}) = \zeta^{\text{LPM}} g \times (ET_{\varepsilon}^3)^{1/4}$
 - $\Lambda_{\perp}^{\text{kin}}(E, T_{\varepsilon}) = \zeta^{\text{kin}} g \times (ET_{\varepsilon})^{1/2}$

- Logarithmic cutoff Λ_{\perp} dependence⁶

$$\hat{q}^{xx}(\Lambda_{\perp} \gg T_{\varepsilon}) \simeq a_x \ln \frac{\Lambda_{\perp}}{Q_s} + b_x$$

(and similar for \hat{q}^{yy})



[Phys.Lett.B 850 (2024) [Boguslavski, Kurkela, Lappi, FL, Peuron]]

Plot for $E = 100 \text{ GeV}$

⁶[Values available at <https://zenodo.org/records/10419537>]

- Cutoff models for dependence on jet energy and effective temperature

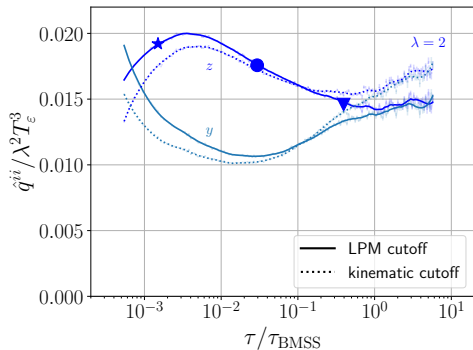
- $\Lambda_{\perp}^{\text{LPM}}(E, T_{\varepsilon}) = \zeta^{\text{LPM}} g \times (ET_{\varepsilon}^3)^{1/4}$

- $\Lambda_{\perp}^{\text{kin}}(E, T_{\varepsilon}) = \zeta^{\text{kin}} g \times (ET_{\varepsilon})^{1/2}$

- Mostly $\hat{q}^{zz} > \hat{q}^{yy}$

→ **Enhanced broadening along beam axis**

- Similar results for both cutoffs



[Phys.Lett.B 850 (2024) [Boguslavski, Kurkela, Lappi, FL, Peuron]]

Plot for $E = 100 \text{ GeV}$

- Cutoff models for dependence on jet energy and effective temperature

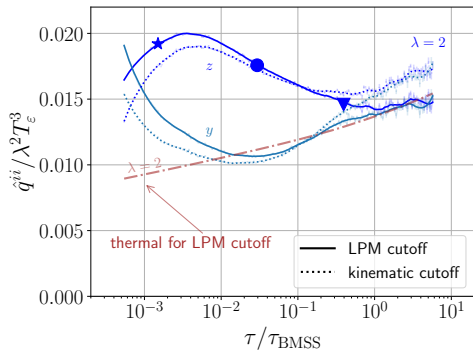
- $\Lambda_{\perp}^{\text{LPM}}(E, T_{\varepsilon}) = \zeta^{\text{LPM}} g \times (ET_{\varepsilon}^3)^{1/4}$

- $\Lambda_{\perp}^{\text{kin}}(E, T_{\varepsilon}) = \zeta^{\text{kin}} g \times (ET_{\varepsilon})^{1/2}$

- Mostly $\hat{q}^{zz} > \hat{q}^{yy}$

→ **Enhanced broadening along beam axis**

- Similar results for both cutoffs



[Phys.Lett.B 850 (2024) [Boguslavski, Kurkela, Lappi, FL, Peuron]]

Plot for $E = 100 \text{ GeV}$

- Cutoff models for dependence on jet energy and effective temperature

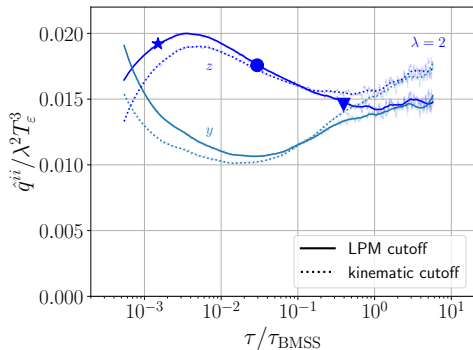
- $\Lambda_{\perp}^{\text{LPM}}(E, T_{\varepsilon}) = \zeta^{\text{LPM}} g \times (ET_{\varepsilon}^3)^{1/4}$

- $\Lambda_{\perp}^{\text{kin}}(E, T_{\varepsilon}) = \zeta^{\text{kin}} g \times (ET_{\varepsilon})^{1/2}$

- Mostly $\hat{q}^{zz} > \hat{q}^{yy}$

→ **Enhanced broadening along beam axis**

- Similar results for both cutoffs

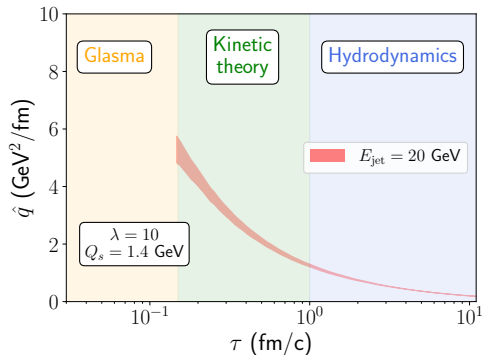


[Phys.Lett.B 850 (2024) [Boguslavski, Kurkela, Lappi, FL, Peuron]]

Plot for $E = 100 \text{ GeV}$

Time evolution of jet quenching parameter

- Model cutoff variation for fixed jet energy
- Dependence on initial conditions and cutoff (bands)

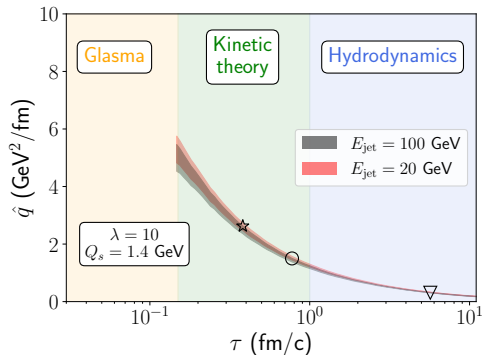


[Phys.Lett.B 850 (2024) [Boguslavski, Kurkela, Lappi, FL, Peuron]]

⁶[Phys.Lett.B 810 (2020) [Ipp, Müller, Schuh]]

Time evolution of jet quenching parameter

- Model cutoff variation for fixed jet energy
- Dependence on initial conditions and cutoff (bands)
- Little jet energy dependence

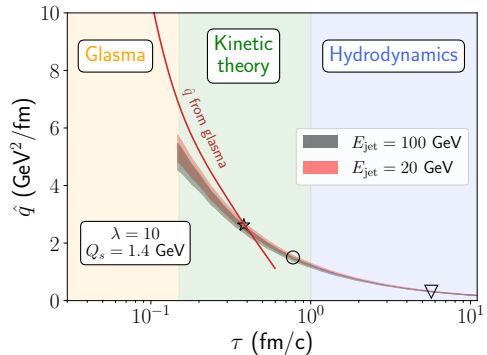


[Phys.Lett.B 850 (2024) [Boguslavski, Kurkela, Lappi, FL, Peuron]]

⁶[Phys.Lett.B 810 (2020) [Ipp, Müller, Schuh]]

Time evolution of jet quenching parameter

- Model cutoff variation for fixed jet energy
- Dependence on initial conditions and cutoff (bands)
- Little jet energy dependence
- Supports **large values** from **Glasma**⁶ and lower values in hydrodynamic stage



[Phys.Lett.B 850 (2024) [Boguslavski, Kurkela, Lappi, FL, Peuron]]

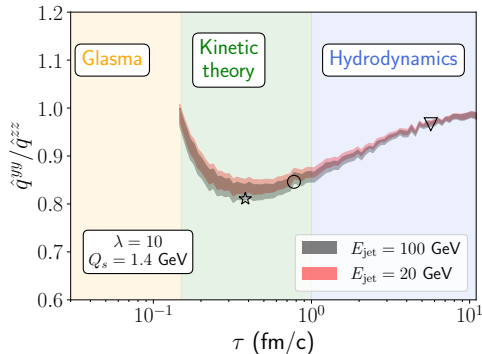
⁶[Phys.Lett.B 810 (2020) [Ipp, Müller, Schuh]]

Time evolution of jet quenching parameter

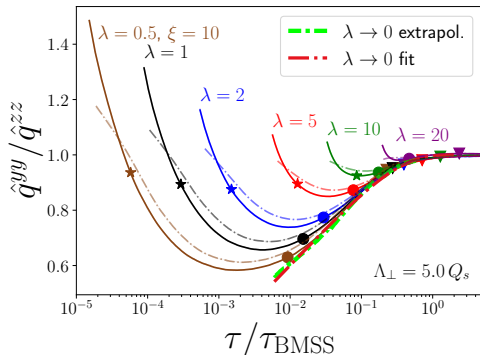
- Model cutoff variation for fixed jet energy
- Dependence on initial conditions and cutoff (bands)
- Little jet energy dependence
- Broadening **anisotropy** up to 15 %
- Possible impact on polarization⁶, azimuthal and spin observables⁷

⁶[JHEP 08 (2023) [Hauksson, Iancu]]

⁷[arXiv:2407.04774 [Barata, Salgado, Silva]]



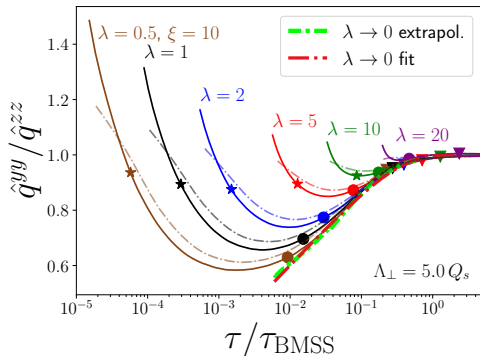
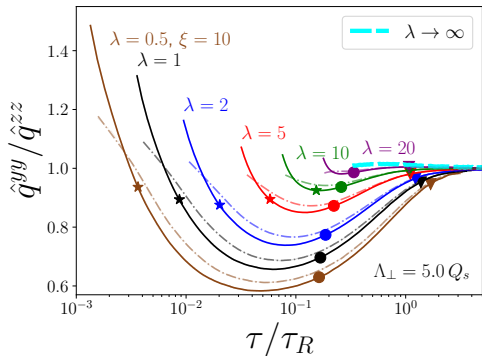
[Phys.Lett.B 850 (2024) [Boguslavski, Kurkela, Lappi, FL, Peuron]]



- Different time scales associated with

$$\text{bottom-up thermalization } \tau_{\text{BMSS}} = \alpha_s^{-13/5} / Q_s$$

- Weak coupling (bottom-up) attractor important already at moderate λ



- Different time scales associated with hydrodynamical attractor $\tau_R = \frac{4\pi\eta/s}{T}$ and bottom-up thermalization $\tau_{\text{BMSS}} = \alpha_s^{-13/5} / Q_s$
- Weak coupling (bottom-up) attractor important already at moderate λ

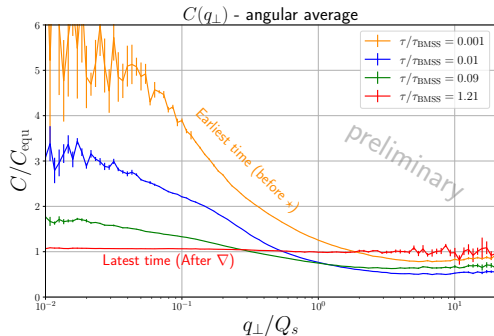
$$C(\mathbf{q}_\perp) = \int d\Gamma_{\text{PS}} |\mathcal{M}|^2 f(\mathbf{k})(1 + f(\mathbf{k} - \mathbf{q}))$$

Normalize using (Landau-matched) thermal kernel, with small q_\perp form⁸

$$C_{\text{equ}}(q_\perp \ll T) = \frac{C_R g^2 T m_D^2}{q_\perp^2 (q_\perp^2 + m_D^2)}$$

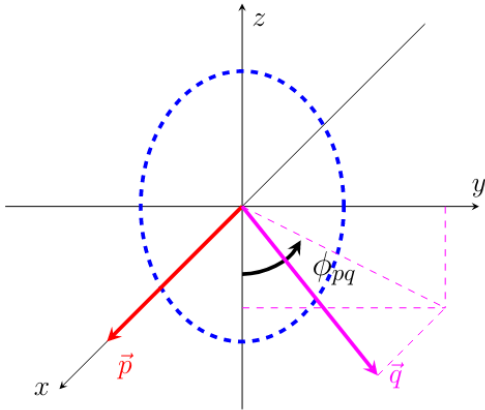
- Momentum transfer of soft momenta enhanced
- Late times (red curve): Thermal

⁸[JHEP 05 (2002) [Aurenche, Gelis, Zaraket]]



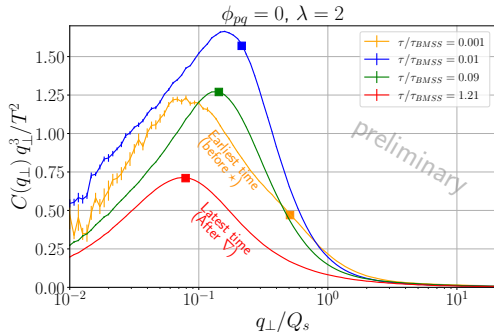
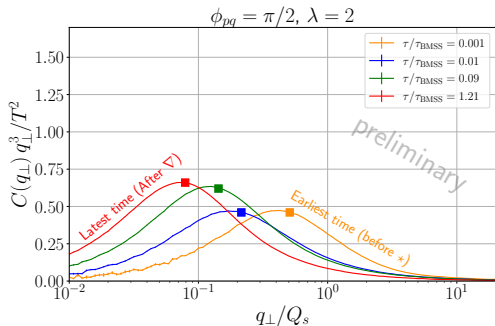
Here, $\lambda = 2$.

Angular dependence and contribution to \hat{q}



- Consider **Angular dependence**
- $\phi_{pq} = 0 \rightarrow$ along beam axis

Angular dependence and contribution to \hat{q}



- Contribution to $\hat{q} = \int d^2\mathbf{q}_\perp q_\perp^2 C(\mathbf{q}_\perp)/(2\pi)$
- **Peaked at Debye mass** ■ for later times
- Along beam ($\phi_{pq} = 0$): Much larger and different form at early times

Conclusions and outlook

- Studied **momentum broadening of jets**
→ \hat{q} and $C(\mathbf{q}_\perp)$ during initial stages in heavy-ion collisions
- Values of \hat{q} within $\sim 20\%$ of thermal estimate
- \hat{q} from kinetic theory **supports large Glasma values**
- More momentum broadening along the beam axis ($\hat{q}^{zz} > \hat{q}^{yy}$)
- $C(\mathbf{q}_\perp)$ at small \mathbf{q}_\perp is enhanced compared to thermal (especially along beam)

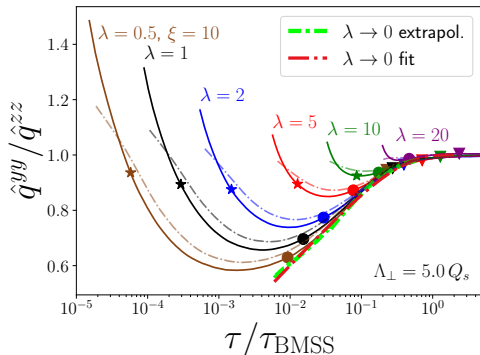
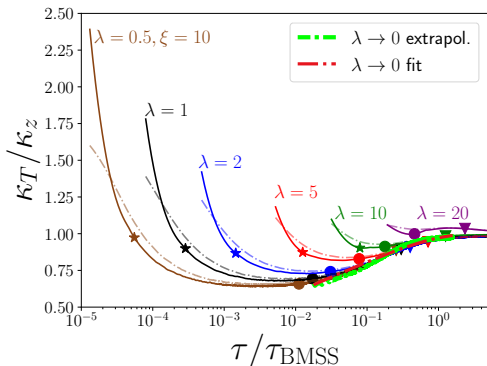
Outlook

- Obtain gluon emission spectrum from pre-equilibrium \hat{q} (with Barata, Sadofyev)
- Inclusion of quarks in plasma background (with Mazeliauskas, Takacs, Zhou)

[Code and data: <https://zenodo.org/records/10419537>, <https://zenodo.org/records/10409474>]

Thank you very much for your attention!

FL is a recipient of a DOC Fellowship of the Austrian Academy of Sciences at the University TU Wien. This work is supported by the Austrian Science Fund (FWF) under project DOI 10.55776/P34455 and 10.55776/W1252



- Approach to universal curve when scaled with $\tau_{\text{BMSS}} = \alpha^{-13/5} / Q_s$
- Many quantities plotted as function of different time ...

Bottom-up vs. hydrodynamic attractor

- Often universal behavior in τ/τ_R ,

$$\tau_R = \frac{4\pi\eta/s}{T}$$

- Conformal (first order) relativistic hydrodynamics ⁹:

$$\frac{P_L}{P_T} = 1 - 8 \underbrace{\frac{\eta/s}{\tau T}}_{\sim \tau_R/\tau}$$

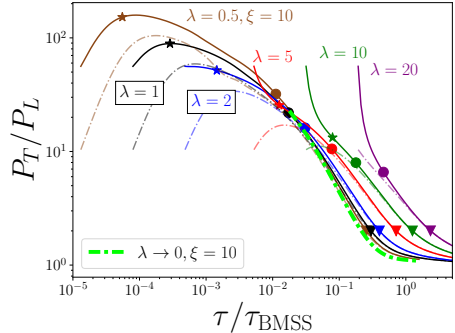
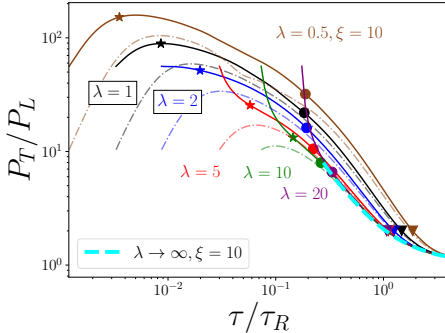
Two different pictures emerge:

- **Bottom-up** expects thermalization around $\tau_{\text{BMSS}} = \alpha_s^{-13/5}/Q_s$
- **Hydrodynamics** expects thermalization around $\tau_R = \frac{4\pi\eta/s}{T}$

⁹[[Romatschke, Romatschke] (2019)]

$$\tau_R = \frac{4\pi\eta/s}{T}, \quad \tau_{\text{BMSS}} = \alpha_s^{-13/5} / Q_s$$

- Kinetic theory simulations for different couplings $0.5 \leq \lambda \leq 20$ and initial conditions.



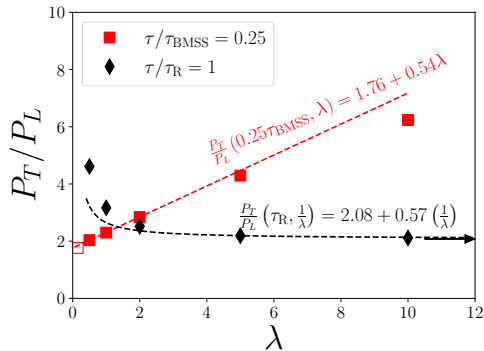
- Attractor for each λ (insensitive to IC)
- Curves approach limiting attractors after •

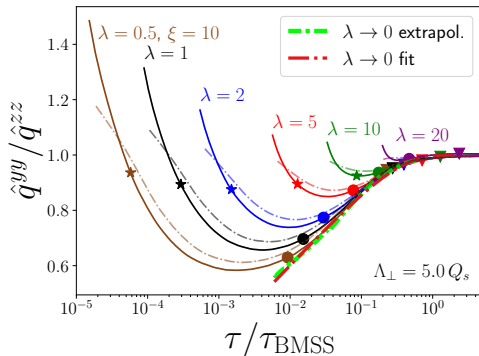
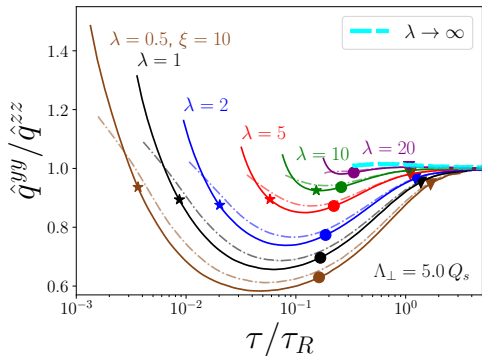
Extrapolation to limiting attractors

$$\tau_R = \frac{4\pi\eta/s}{T}$$

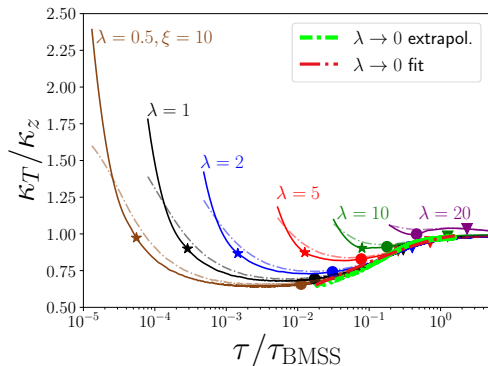
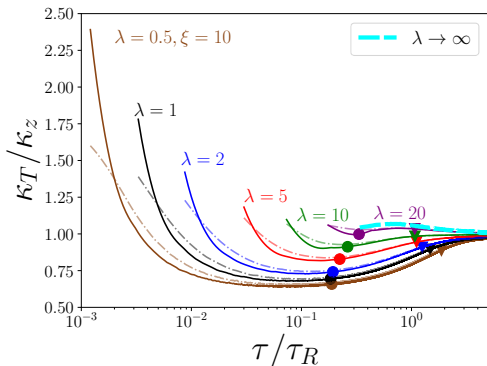
$$\tau_{\text{BMSS}} = \alpha_s^{-13/5} / Q_s$$

- Obtain limiting attractors by extrapolating at fixed τ/τ_R or τ/τ_{BMSS}
- **Bottom-up attractor**: Linear extrapolation to $\lambda \rightarrow 0$
- **Hydro attractor**: Linear extrapolation to $1/\lambda \rightarrow 0$





- Approach to weak coupling attractor even at moderate couplings



- Similar to \hat{q} : Approach to weak coupling attractor even at moderate λ

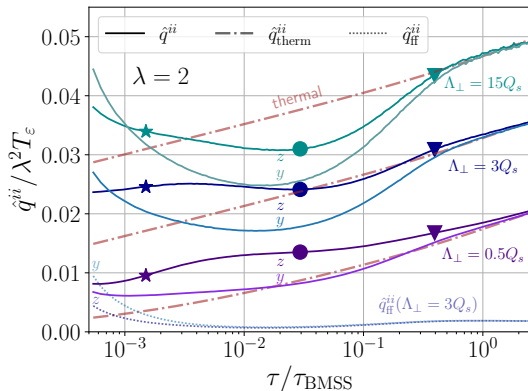
- \hat{q} for fixed coupling $\lambda = 2$ and varying cutoffs Λ_{\perp}

- 2D distribution

$$f(\mathbf{k}) \sim \delta(k_z)$$

Leads to $\hat{q}_{\text{ff}}^{zz} = 0$

- Reason for different ordering:
Bose-enhanced part \hat{q}_{ff} = term quadratic in $f(\mathbf{k})$



Screening in the matrix element of \hat{q}

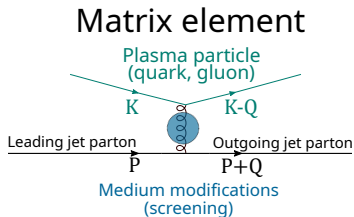
- Scattering matrix element includes **in-medium propagator**
- Receives **self-energy corrections**
- Anisotropic hard thermal loop (HTL) self-energy \rightarrow unstable modes¹⁰
- **Approximation: Use isotropic HTL matrix element**

Similar approximation also in EKT implementations¹¹

¹⁰[Phys.Rev.D 68 (2003) [Romatschke, Strickland]]

¹¹[Phys.Rev.Lett. 115 (2015) [Kurkela, Zhu]; Phys.Rev.Lett. 122 (2019) [Kurkela, Mazeliauskas];

Phys.Rev.D 104 (2021) [Du, Schlichting]]

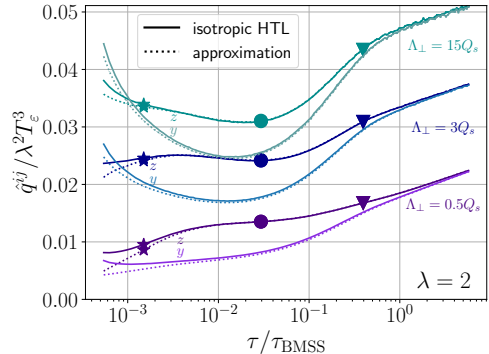


Screening approximation to the matrix element

- Compare with simple screening approximation

$$\frac{(s-u)^2}{t^2} \rightarrow \frac{(s-u)^2}{t^2} \frac{q^4}{(q^2 + \xi_T^2 m_D^2)^2}$$

- Longitudinal¹² $\xi_L = e^{5/6}/\sqrt{8}$
- Transverse broadening:
 $\xi_T = e^{1/3}/2$
- **Good agreement**

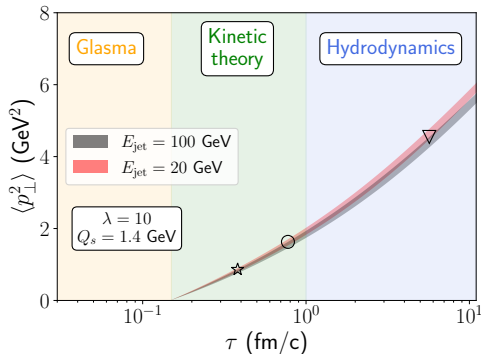


s, u, t : Mandelstam variables

¹²[Phys.Rev.D 89 (2014) [York, Kurkela, Lu, Moore]]

What about total momentum broadening?

- Per definition, $\hat{q} = \frac{d\langle p_{\perp}^2 \rangle}{d\tau}$
- Naively $\Delta p_{\perp}^2 = \int d\tau \hat{q}(\tau)$ over lifetime of jet
- Think of \hat{q} as medium parameter.



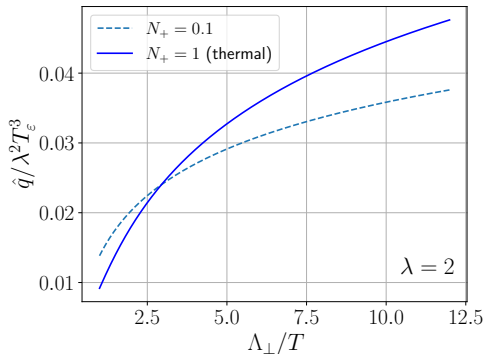
- Scaled thermal distribution

$$f(k; T) = \frac{N_+}{\exp(k/T) - 1}$$

Explains ordering $\hat{q}_{\text{therm}} \lesssim \hat{q}$ for underoccupancy

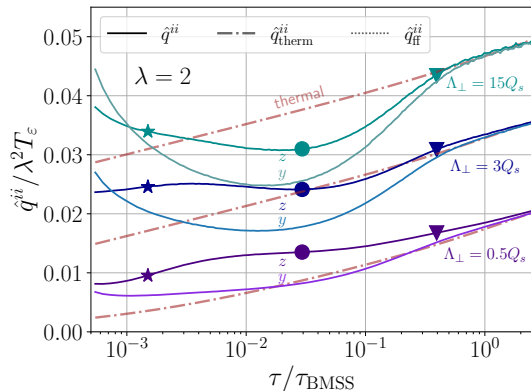
[arXiv:2312.00447 [Boguslavski, Kurkela, Lappi, FL, Peuron]]

Scaled thermal distribution



Cutoff dependence and comparison with equilibrium

- \hat{q} for fixed coupling $\lambda = 2$ and varying cutoffs Λ_{\perp}
- Ordering $\hat{q}^{yy} \lesseqgtr \hat{q}^{zz}$ depends on cutoff
- Energy-matched equilibrium over- or underestimates \hat{q} , depending on cutoff



Making sense of the cutoff

- Cutoff Λ_{\perp} restricts transverse momentum transfer $q_{\perp} < \Lambda_{\perp}$
(needed in eikonal limit $p \rightarrow \infty$)

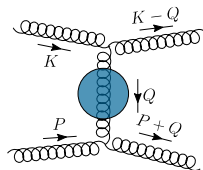
$$\hat{q} \sim \int d^2 q_{\perp} q_{\perp}^2 \underbrace{\frac{d\Gamma^{\text{el}}}{d^2 q_{\perp}}}_{1/q_{\perp}^4 \text{ for large } q_{\perp}} \sim \int \frac{dq_{\perp}}{q_{\perp}}$$

Making sense of the cutoff

- Cutoff Λ_{\perp} restricts transverse momentum transfer $q_{\perp} < \Lambda_{\perp}$
(needed in eikonal limit $p \rightarrow \infty$)
- Cutoff should grow with jet energy
- **kinematic cutoff** $\Lambda_{\perp}^{\text{kin}}(E, T) = \zeta^{\text{kin}} g(ET)^{1/2}$
obtained from comparing leading log behavior for large p and Λ_{\perp}
- **LPM cutoff** $\Lambda_{\perp}^{\text{LPM}}(E, T) = \zeta^{\text{LPM}} g(ET^3)^{1/4}$
Estimate for momentum broadening during LPM 'formation time':
 $Q_{\perp}^2 \sim \hat{q} t^{\text{form}}, t^{\text{form}} \sim \sqrt{E/\hat{q}},$ approximately $\hat{q} \sim g^4 T^3$

[arXiv:2312.00447 [Boguslavski, Kurkela, Lappi, FL, Peuron]]

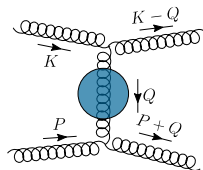
$$C^{2\leftrightarrow 2}[f(\mathbf{p})] = \int_{\mathbf{k}\mathbf{k}'} |\mathcal{M}(\mathbf{p}, \mathbf{k}; \mathbf{p}'\mathbf{k}')|^2 \left\{ f_{\mathbf{p}} f_{\mathbf{k}} [1 + f_{\mathbf{p}'}] [1 + f_{\mathbf{k}'}] - f_{\mathbf{p}'} f_{\mathbf{k}'} [1 + f_{\mathbf{p}}] [1 \pm f_{\mathbf{k}}] \right\},$$



$$C^{2\leftrightarrow 2}[f(\mathbf{p})] = \int_{\mathbf{k}\mathbf{k}'} |\mathcal{M}(\mathbf{p}, \mathbf{k}; \mathbf{p}', \mathbf{k}')|^2 \left\{ f_{\mathbf{p}} f_{\mathbf{k}} [1 + f_{\mathbf{p}'}] [1 + f_{\mathbf{k}'}] - f_{\mathbf{p}'} f_{\mathbf{k}'} [1 + f_{\mathbf{p}}] [1 \pm f_{\mathbf{k}}] \right\},$$

with medium effects included in the **vaccum matrix element**

$$\frac{|\mathcal{M}|^2}{4\lambda^2 d_A} = 9 + \frac{(s-t)^2}{\underline{u}^2} + \frac{(u-s)^2}{\underline{t}^2} + \frac{(t-u)^2}{s^2}.$$



Elastic collision term

$$C^{2\leftrightarrow 2}[f(\mathbf{p})] = \int_{\mathbf{k}\mathbf{k}'} |\mathcal{M}(\mathbf{p}, \mathbf{k}; \mathbf{p}', \mathbf{k}')|^2 \left\{ f_{\mathbf{p}'} f_{\mathbf{k}} [1 + f_{\mathbf{p}}] [1 + f_{\mathbf{k}'}] - f_{\mathbf{p}} f_{\mathbf{k}'} [1 + f_{\mathbf{p}'}] [1 \pm f_{\mathbf{k}}] \right\},$$

with medium effects included in the **vaccum matrix element**

$$\frac{|\mathcal{M}|^2}{4\lambda^2 d_A} = 9 + \frac{(s-t)^2}{\underline{u}^2} + \frac{(u-s)^2}{\underline{t}^2} + \frac{(t-u)^2}{s^2}.$$

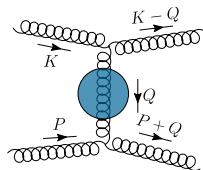
via the replacement (“**Debye-like screening**”)

$$\frac{(u-s)^2}{\underline{t}^2} \rightarrow \frac{(u-s)^2}{t^2} \frac{q^4}{(q^2 + \xi^2 m_D^2)^2},$$

$$\xi = e^{5/6} / \sqrt{8}$$

m_D ... Debye mass

s, u, t ... Mandelstam variables



as simple **isotropic approximation** for **hard thermal loop propagator**.

[Phys.Rev.D 89 (2014) [Abraao York, Kurkela, Lu, Moore]]

$$\partial_\tau f = -\mathcal{C}^{2\leftrightarrow 2} - \mathcal{C}^{1\leftrightarrow 2}$$

$$\mathcal{C}^{2\leftrightarrow 2}[f(\mathbf{p})] = \int_{\mathbf{k}\mathbf{k}'} |\mathcal{M}(\mathbf{p}, \mathbf{k}; \mathbf{p}'\mathbf{k}')|^2 \left\{ f_{\mathbf{p}} f_{\mathbf{k}} [1 + f_{\mathbf{p}'}] [1 + f_{\mathbf{k}'}] - f_{\mathbf{p}'} f_{\mathbf{k}'} [1 + f_{\mathbf{p}}] [1 \pm f_{\mathbf{k}}] \right\},$$

with medium effects included in the vacuum matrix element

$$\frac{|\mathcal{M}|^2}{4\lambda^2 d_A} = 9 + \frac{(s-t)^2}{\underline{u}^2} + \frac{(u-s)^2}{\underline{t}^2} + \frac{(t-u)^2}{s^2}.$$

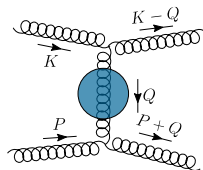
via the replacement (“**Debye-like screening**”)

$$\frac{(u-s)^2}{\underline{t}^2} \rightarrow \frac{(u-s)^2}{t^2} \frac{q^4}{(q^2 + \xi^2 m_D^2)^2},$$

$$\xi = e^{5/6} / \sqrt{8}$$

m_D ... Debye mass

s, u, t ... Mandelstam variables



as simple **isotropic approximation** for **hard thermal loop propagator**.

[Phys. Rev. D 89 (2014) [Abraao, York, Kurkela, Lu, Moore]]

$$\partial_\tau f = -\mathcal{C}^{2\leftrightarrow 2} - \mathcal{C}^{1\leftrightarrow 2}$$

$$\mathcal{C}^{2\leftrightarrow 2}[f(\mathbf{p})] = \int_{\mathbf{k}\mathbf{k}'} |\mathcal{M}(\mathbf{p}, \mathbf{k}; \mathbf{p}'\mathbf{k}')|^2 \left\{ f_{\mathbf{p}} f_{\mathbf{k}} [1 + f_{\mathbf{p}'}] [1 + f_{\mathbf{k}'}] - f_{\mathbf{p}'} f_{\mathbf{k}'} [1 + f_{\mathbf{p}}] [1 \pm f_{\mathbf{k}}] \right\},$$

with medium effects included in the vacuum matrix element

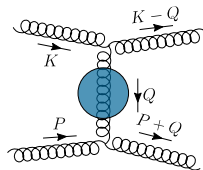
$$\frac{|\mathcal{M}|^2}{4\lambda^2 d_A} = 9 + \frac{(s-t)^2}{\underline{u}^2} + \frac{(u-s)^2}{\underline{t}^2} + \frac{(t-u)^2}{s^2}.$$

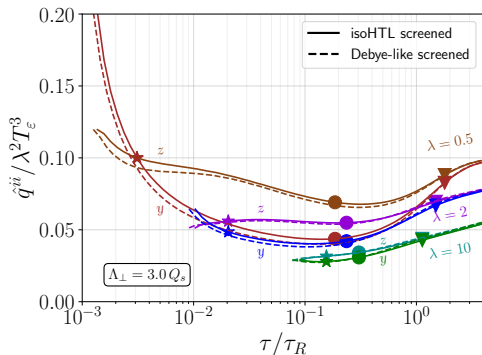
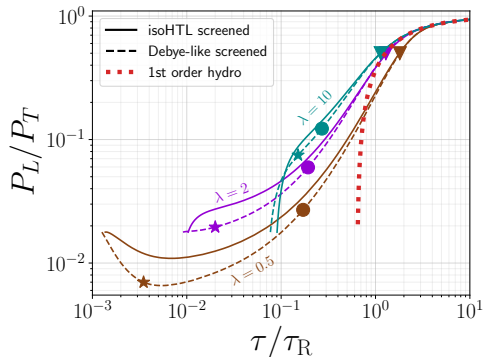
via the replacement (“**isoHTL screening**”)

$$\frac{(u-s)^2}{\underline{t}^2} \rightarrow \left| G_{\mu\nu}^{\text{HTL,ret}}(P - P') (P + P')^\mu (K + K')^\nu \right|^2$$

with G the **isotropic hard thermal loop propagator**.

[JHEP 01 (2003) [Arnold, Moore, Yaffe], arXiv:2407.09605 [Boguslavski, FL]]





- Left: Screening affects pressure ratio at early times
- Right: Minimal effect on \hat{q}